



Science Arts & Métiers (SAM)

is an open access repository that collects the work of Arts et Métiers Institute of Technology researchers and makes it freely available over the web where possible.

This is an author-deposited version published in: <https://sam.ensam.eu>
Handle ID: [.http://hdl.handle.net/10985/15196](http://hdl.handle.net/10985/15196)

To cite this version :

Zimo WANG, Satish BUKKAPATNAM, Mohamed EL MANSORI, Faissal CHEGDANI - Multiscale tribo-mechanical analysis of natural fiber composites for manufacturing applications - Tribology International - Vol. 122, p.143-150 - 2018

Any correspondence concerning this service should be sent to the repository

Administrator : scienceouverte@ensam.eu



Multiscale tribo-mechanical analysis of natural fiber composites for manufacturing applications

Faissal Chegdani^{a,b,*}, Zimo Wang^a, Mohamed El Mansori^b, Satish T.S. Bukkapatnam^a

^a Texas A&M University, Department of Industrial and Systems Engineering, 3131 TAMU, College Station, TX 77843, USA

^b Arts et Métiers ParisTech, MSMP Laboratory / EA7350, Rue Saint Dominique BP508, Châlons-en-Champagne, 51006, France

ARTICLE INFO

Keywords:

Natural fiber composites
Nanoindentation
Scratch test
Multiscale friction

ABSTRACT

This paper aims to investigate the tribo-mechanical behavior of natural fiber reinforced plastic (NFRP) composites with specific consideration of the multiscale complex structure of natural fibers. Understanding the multiscale tribo-mechanical performances of these eco-friendly materials can lead to a better design of their manufacturing processes. Nanoindentation and nanoscratching experiments are conducted on flax fibers reinforced polypropylene composites using a triboindenter at a specific contact scale generated by the tip indenter radius (100 nm). Results confirm the significant effect of the geometric contact scale on the flax fibers stiffness. Moreover, flax fibers friction shows a multiscale behavior where the mechanisms of nano-friction are vastly different from those of micro-friction, which is related to the physical phenomena arisen at each scale.

1. Introduction

Natural fibers reinforced plastic (NFRP) composites are increasingly used in different industry fields due to their many economic, ecological and technical advantages [1–6]. Indeed, natural fibers are biodegradable and recyclable [7]. Their industrial use can promote circular economy and sustainable development. Moreover, some natural fibers, especially plant fibers such as flax, hemp or jute, have good mechanical performances which can compete with that of glass fibers commonly used in industry [2,8]. Therefore, manufacturing processes to translate these eco-friendly materials for industrial applications are gaining notable interest [9]. Among the manufacturing processes, machining of composite materials is essential to achieve the geometric quality specifications for industrial parts [10].

NFRP composites pose significant machinability issues because natural fibers are themselves heterogeneous with high transversal flexibility [11–14]. In fact, natural fibers are themselves a composite material with a cellulosic structure in form of cellulose microfibrils along the fibers axis [15,16]. Therefore, NFRP composites involve a multiscale heterogeneity from microscopic elementary fiber scale to the overall macroscopic NFRP composite scale which has a significant impact on the tribological cutting behavior of natural fibers within NFRPs [11–13]. Moreover, it has been reported that NFRP composites have specific tribological performances where the incorporation of natural fibers into polymer matrix improves

the macroscopic tribological behavior by increasing the wear resistance and reducing the friction coefficient of the NFRPs [17–22].

In this context, our previous work has investigated the contact scale effect on the tribo-mechanical behavior of NFRP composites by changing the contact scale during nanoindentation experiments [23]. It shows that natural fibers present a scale effect in terms of mechanical properties where the fiber stiffness is intimately dependent on the geometric contact scale. Moreover, the friction behavior of NFRP composites differs from fibers to the matrix and this difference is intimately related to the micro-mechanical behavior of each NFRP constituent at the same contact scale. These findings are important outcomes that can allow a better understanding of the multiscale cutting behavior shown on NFRP composites during finishing operations [11–14]. Indeed, the mechanical contact behavior between the tip indenter and the NFRP material can be assimilated to the contact between the abrasive polishing grain and the NFRP worksurface. Also, this tribo-mechanical approach can be extrapolated to the machining contact behavior between the cutting tool edge and the NFRP material at the beginning of the cutting engagement. Understanding the multiscale tribo-mechanical behavior of NFRPs can lead to a better comprehension of machining performances of these eco-friendly materials and, thereby, improve their machinability.

However, the scale effect shown on NFRP mechanical properties [23] is not yet investigated for the tribological properties of NFRP composites. Scratch test in Ref. [23] has been made at only one contact scale that was

* Corresponding author. Texas A&M University, Department of Industrial and Systems Engineering, 3131 TAMU, College Station, TX 77843, USA.
E-mail address: faissal.chegdani@ensam.eu (F. Chegdani).

performed by atomic force microscopy (AFM) using a diamond tip indenter. Therefore, the effect of changing the geometric contact scale on the friction behavior of natural fibers inside composite materials is still not well understood. This causes unfortunately a significant lack of understanding the tribological cutting behavior of these multiscale materials during machining operations.

Towards addressing this gap, this paper performs a tribo-mechanical investigation of the local behavior of flax fiber-reinforced polypropylene composites at a geometric contact scale that is different from those investigated in Ref. [23]. The purpose of this work is to broaden the understanding of the multiscale tribo-mechanical behavior for natural fibers inside composite materials. This will allow a better prediction of the complex material removal mechanisms of NFRP composites. In this work, a triboindenter is used to conduct both nanoindentation and scratch tests on NFRP composites surface by soliciting the elementary flax fibers and the polypropylene matrix separately at a microscale. Nanoindentation tests are used to reveal the local material stiffness while scratch tests are performed to determine the local friction response. The geometric contact scale is generated by the indenter tip radius.

2. Material and methods

NFRP composite samples used in this study (Fig. 1(a)) are manufactured and supplied by “Composites Evolution – UK” and are composed of unidirectional flax fibers (40% vt) as fiber yarns commingled with polypropylene (PP) matrix (60 %vt). Flax fibers are perpendicular to the worksurface and are randomly distributed as presented in Fig. 1(b) that

shows the variability aspect known for natural fibers. In addition, Fig. 1(b) reveals that flax fibers are either separated into single fibers (called elementary fibers) or bundles of single fibers (called technical fibers) inside the PP matrix. Obviously, flax elementary fibers have random shapes and diameters. However, the typical elementary shape is assumed polygonal and the fibers diameter is between 10 μm and 20 μm as illustrated in Fig. 1(c). Indeed, A typical elementary fiber consists of a stack of two cell walls with a small channel in the middle called lumen [15] (see Fig. 1(c)). Each cell wall is itself a composite of cellulose microfibrils and non-cellulosic polymer [16]. All the NFRP worksurfaces are polished with the same grit size (~3 μm) to have the same initial conditions for nanoindentation and scratch tests.

Both nanoindentation and scratch tests are performed on Hysitron nanoindenter (model TI-950) with Berkovich diamond tip indenter (model TI-0039). The relevant parameter of this indenter model is its tip radius which is around 100 nm. Indeed, the considered tip radius value is between the values of those used in Ref. [23] (40 nm for AFM tip indenter and 400 nm for MTS tip indenter). Since these two previous tip indenters are also Berkovich diamond type, the comparison of the mechanical scales generated by these three tip radius values (40 nm, 100 nm and 400 nm) can be pertinent.

For nanoindentation tests, the tip indenter penetrates the worksurface to reach a specific load or depth (Fig. 2(a)). Then, the load is measured as a function of the penetration depth and the resulting curve is used to calculate the elastic modulus of the studied material. Indeed, the load-penetration curve gives the pertinent parameters to analyze the mechanical response as shown in Fig. 3. Here, the maximum displacement

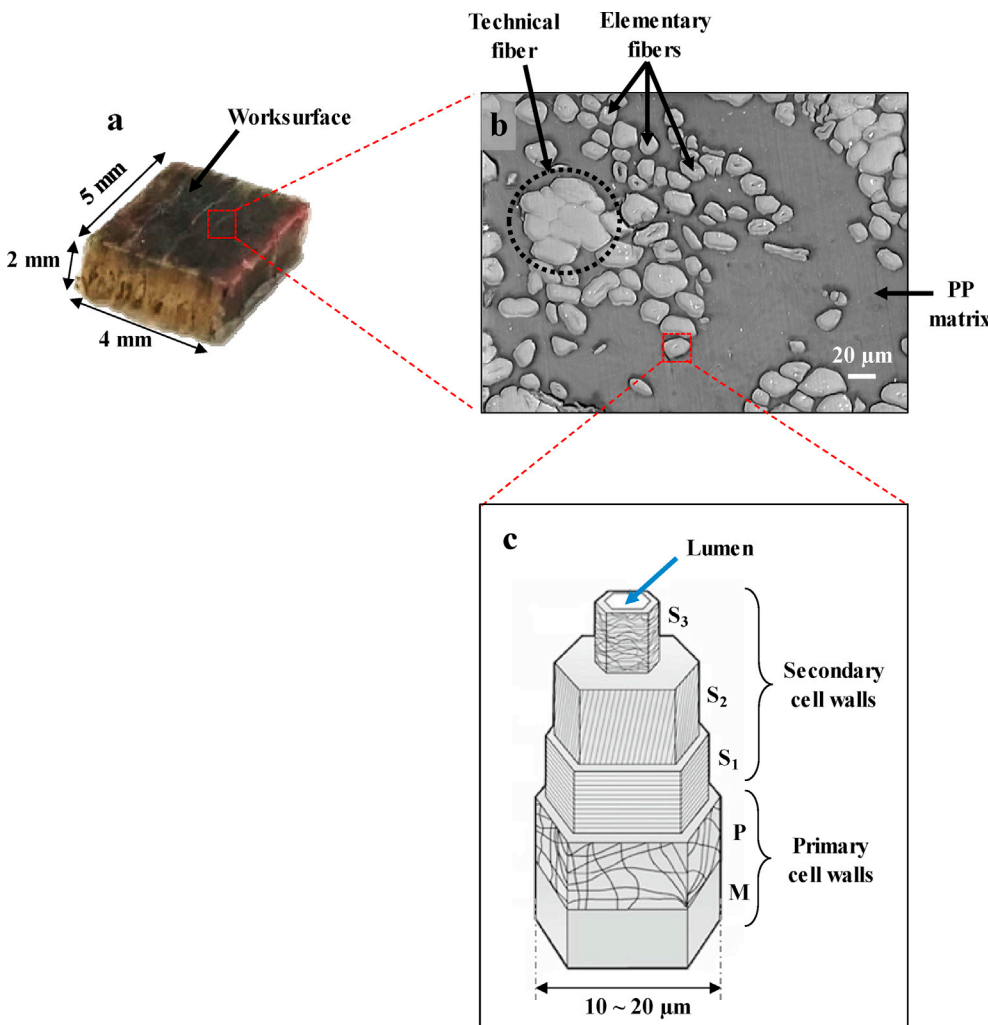


Fig. 1. a) Photograph of flax/PP workpiece. b) SEM image of the flax/PP worksurface. c) Schematic depiction of elementary flax fiber [9].

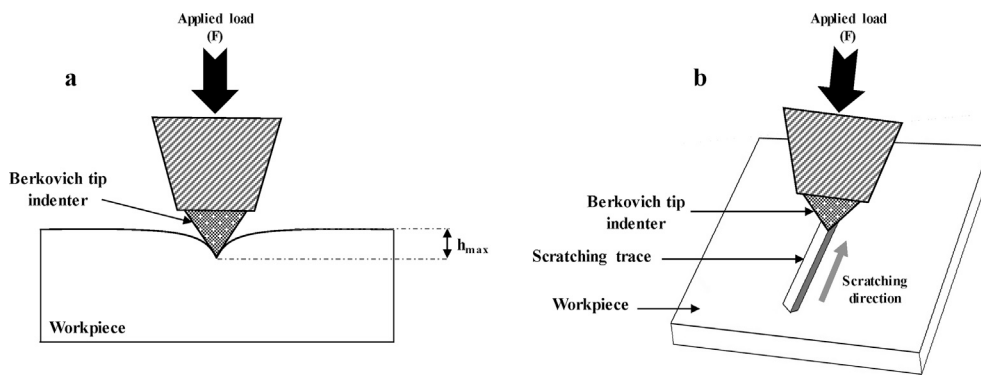


Fig. 2. Schematic depiction of (a) nanoindentation tests, and (b) scratch tests.

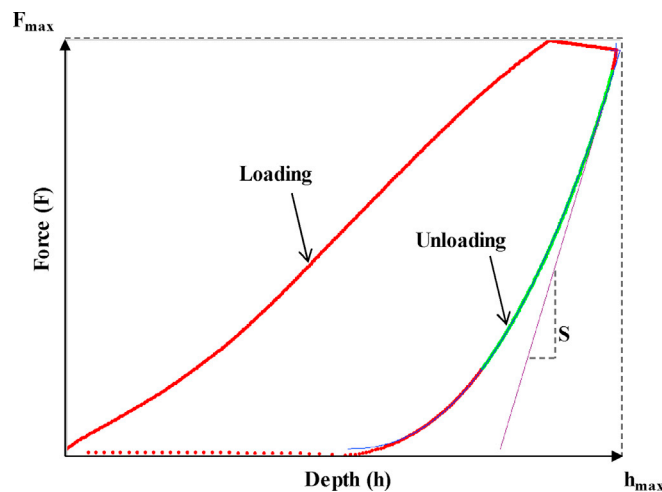


Fig. 3. Typical load-penetration curve from nanoindentation showing the relevant parameters for elastic modulus calculation.

(h_{max}), the maximum load (F_{max}) and the contact stiffness (S), which is the slope of the tangent line to the unloading curve at the maximum loading point, are the three relevant parameters to calculate the elastic modulus following the model of Oliver & Pharr [24]. The calculation procedure is detailed by the authors in Ref. [23]. A large range of applied load values is considered to generate different contact depth values (See Table 1).

For scratch tests, the tip indenter slides on the worksurface with a specific load, speed, and length (Fig. 2(b)). The in-situ normal and lateral forces are measured and the dynamic friction coefficient (μ_D) is calculated as the ratio between the lateral force and the normal force. The considered scratching length is 10 μm in order to work on elementary flax fibers and PP matrix separately. Table 1 presents the considered nanoindentation and scratch tests conditions for this study.

Table 1
Considered parameters for nanoindentation and scratch tests.

	Nanoindentation	Scratch test
Applied load (μN)	50 100 200 300 400 500	100 300 500
Sliding speed ($\mu\text{m/s}$)	-	2 4 6 8 10

3. Results and discussion

3.1. Mechanical properties by nanoindentation

Fig. 4 shows the indentation traces on both elementary flax fibers and PP matrix at the same applied load (500 μN). The images are obtained by scanning probe microscopy (SPM) mode included in the nanoindenter. The considered images are based on the measured interaction force between the tip indenter and the worksurface molecules. This SPM mode can reveal the microscopic surface morphology. The maximum indentation trace size of both flax fibers and PP matrix are measured and are around $1.37^{\pm 0.25} \mu\text{m}$ for flax fibers, and $2.25^{\pm 0.23} \mu\text{m}$ for PP matrix. The indentation trace size of PP matrix is greater than that of flax fiber because the penetration depth is higher when indenting on PP matrix as shown in Fig. 5. Moreover, Fig. 5 demonstrates the significant effect of the applied load on the penetration depth because of the viscoelasticity of both PP matrix and flax fibers. Indeed, the viscoelasticity of PP matrix is well known since a long time [25,26]. On the other hand, flax fibers also show a viscoelastic comportment due to the low relaxation times of the non-cellulosic polymers and amorphous cellulose that are responsible for this viscoelastic behavior [27].

Fig. 6 presents the elastic modulus from nanoindentation tests for flax fibers and PP matrix. It can be seen the significant variability of elastic modulus for flax fibers. This is mainly due to the heterogeneous cellulosic structure of flax fibers as explained in Section 2. Therefore, the nanoindentation response of flax fibers is significantly dependent on the nanoindentation location inside the fiber cross-section. Moreover, the elastic modulus of flax fibers decreases significantly by increasing the penetration depth. This is the sign that the amorphous non-cellulosic constituents of flax fibers have the main contribution at this contact scales. Indeed, the cross-section size of cellulose microfibrils is around 1–4 nm, and the cross-section of cellulose mesofibrils (i.e. bundle of microfibrils) is around 100–300 nm [28] which is in the same magnitude as the tip indenter radius (100 nm). As the cellulosic microfibrils are almost perpendicular to the fiber cross-section [15], increasing the contact depth (i.e. increasing the applied load) during nanoindentation makes the cellulose microfibrils transversally deviated from the indentation path. This leads to avoid the contact with cellulosic microfibrils and then favor the contact with the amorphous non-cellulosic polymers (hemicellulose and lignin). Thus, increasing the cutting depth during the indentation generates elastic modulus values near to those of hemicellulose and lignin that are around 3.5–8.0 GPa for hemicellulose and 2–6.7 GPa for lignin [29]. On the other hand, elastic modulus values of PP matrix show neither high variation nor high variability because of its homogeneity.

3.2. Multiscale mechanical behavior of natural fibers

As demonstrated in our previous work [23], the mechanical response of natural fiber depends on the geometric contact scale. However, this

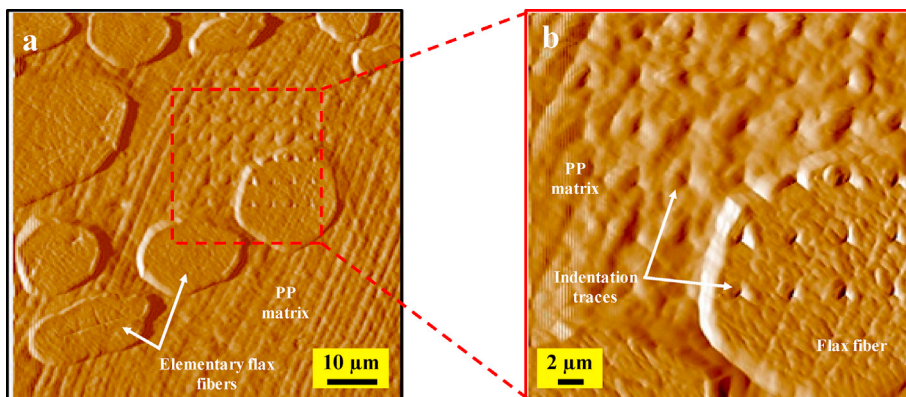


Fig. 4. (a) SPM image on the NFRP worksurface. (b) Zoom on the active zone showing the indentation traces.

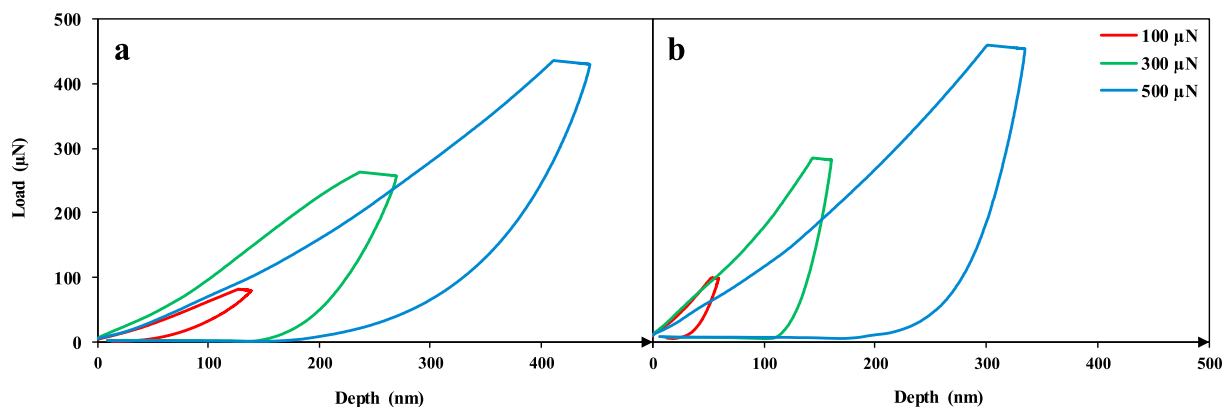


Fig. 5. Typical loading-unloading curves obtained by nanoindentation for (a) PP matrix and (b) flax fibers.

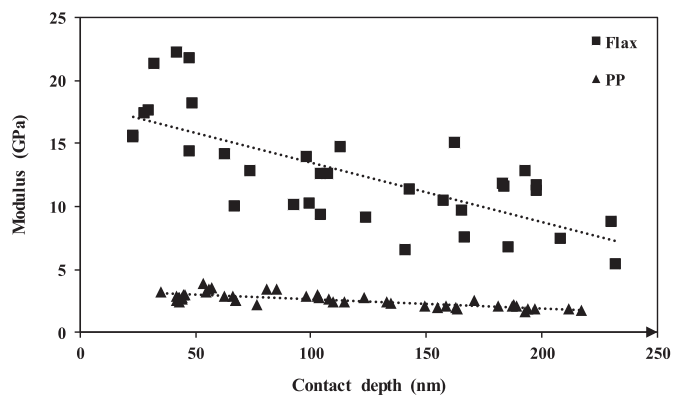


Fig. 6. Elastic modulus values obtained by nanoindentation on flax elementary fibers and PP matrix.

previous work investigated only two geometric contact scales generated using two tip indenter radii (40 nm and 400 nm). Therefore, the relationship between the mechanical response and the geometric contact scale could not be generalized by only two geometric contact conditions. The aim of this section is to compare the previous results to those of this study that are generated with a tip indenter radius of 100 nm and then verify the geometric contact scale impact.

Fig. 7 shows the elastic modulus of both flax fibers and PP matrix performed at iso applied load (500 μN) with the three different tip indenter radii. This comparison confirms the impact of the geometric contact scale on the elastic response of flax fibers. Indeed, there is a drastic increase of the elastic modulus by increasing the tip radius from 40 nm to 100 nm and from 100 nm to 400 nm. However, the elastic

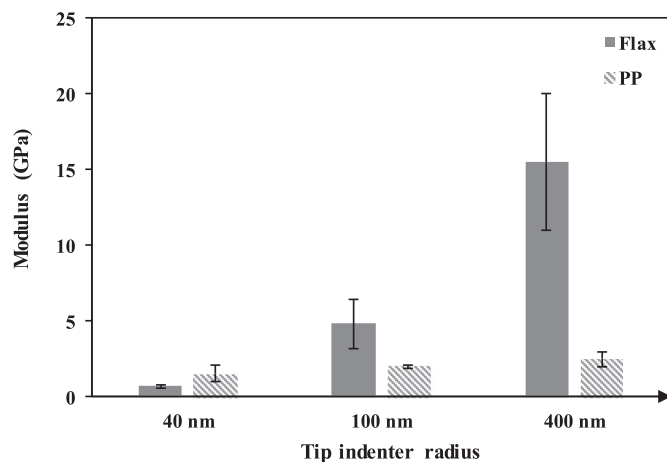


Fig. 7. Comparison of elastic modulus obtained by nanoindentation with the current tip radius (100 nm) and two other tip radius values (40 nm and 400 nm) reproduced from Ref. [23].

response of PP matrix is not affected by changing the geometric contact scale. This is the sign that the multiscale cellulosic structure of natural fibers (microfibrils → mesofibrils → elementary fibers) have a significant impact on their mechanical properties.

Fig. 8 illustrates the effect of the geometric contact scale on the elastic response. When indenting with low tip indenter radius below the mesofibrils diameter (100–300 nm) [28], the cellulose microfibrils (diameters between 1 and 4 nm [28]) are transversally deviated from the indentation path as shown in Fig. 8(a). The mechanical response is almost that of non-cellulosic polymers in contact with the tip indenter.

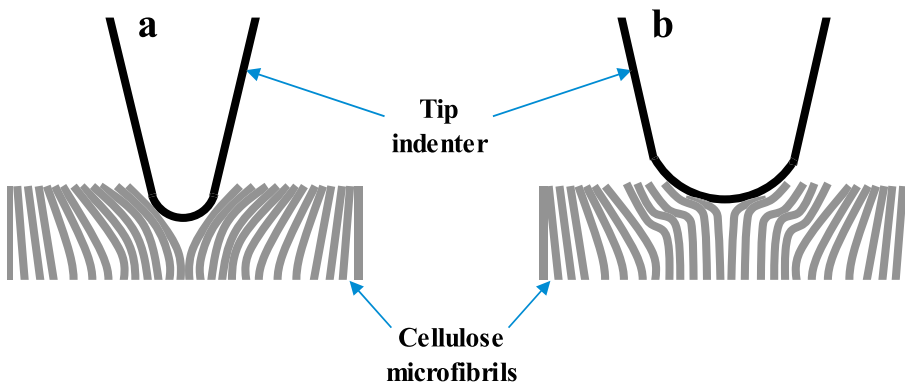


Fig. 8. Schematic depiction of the contact nature between the tip indenter and cellulose microfibrils in natural fibers at (a) low tip radius and (b) high tip radius.

Since the tip indenter radius reaches the mesofibrils size, the indentation operation considers also the microfibrils that have a high stiffness (135 GPa [15]) as shown in Fig. 8(b). Then, the indentation modulus increases by increasing the microfibrils contents in the contact area.

3.3. Friction properties by scratch test

Fig. 9 shows scratching traces performed on flax fibers and PP matrix. Scratching PP matrix generated high plastic deformation, while scratching flax fibers cross-sections seems to generate a material removal without high plastic deformation. Indeed, scratching PP matrix induced an obvious material plastic flow at the borders of the scratching lines as marked in Fig. 9(a). This indicated that scratching PP matrix engenders a ploughing mechanism. For flax fibers scratching, this phenomenon is not noticeable, and the material shearing seems to be the predominant mechanism during scratching. This observation is more apparent at high applied load (500 μN) where the scratching depth is the largest. The difference in the mechanisms that occurred when scratching flax fibers and PP matrix can be due to the high plasticity of PP matrix compared to flax fibers as shown in the nanoindentation study reported in Section 3.1 and Section 3.2.

Fig. 10 illustrates the dynamic friction response of flax fibers cross-sections and PP matrix. Generally, the friction coefficient increases slightly with the sliding speed increase. Flax fibers friction seems not to be affected by the applied load during scratching while PP matrix friction decreases slightly by scratching load increase. Fig. 10 shows that the difference of friction behavior between flax fibers and PP matrix is significantly dependent on the applied load and sliding speed. Indeed, at 100 μN of applied load, there is no significant difference between the friction response of flax fibers and PP matrix (Fig. 10(a)). By increasing the load to 300 μN , the difference starts to be obvious at high sliding speeds (8–10 $\mu\text{m/s}$) where flax fibers generate more friction than PP matrix (Fig. 10(b)). However, at 500 μN of applied load, the friction behavior is well discriminated between flax fibers and PP matrix at larger sliding speed range (4–10 $\mu\text{m/s}$) as shown in Fig. 10(c). At this load levels, the friction response of flax fibers is clearly higher than that of PP matrix.

Friction is a complex phenomenon that cannot be reduced to a single mechanism, but rather is a result of a simultaneous action of various mechanisms at different hierarchy and scale levels [30,31]. To understand this specific friction behavior of the two NFRP constituents, Fig. 11 illustrates the average elastic response performed by nanoindentation at the three applied load values considered for scratching. It can be seen that the elastic modulus of flax fibers drastically decreases when the load increases, while that of PP matrix seems to be not significantly affected by increasing the applied load. This demonstrates the functional relationship between the mechanical properties and the tribological properties of NFRP composites.

The friction behaviors can be explained by the activated mechanisms during the scratch that are related to the mechanical properties of each

NFRP constituent. For PP matrix, the applied load does not affect the mechanical response. Therefore, the applied load will not affect significantly the friction force. Since the friction coefficient is the ratio between the friction force and the normal force (i.e. the applied load) and the friction force is not strongly affected by the applied load, the friction coefficient should decrease by increasing the applied load. Consequently, the well-known micro-friction behavior of polypropylene is found where the friction coefficient decreases with the load increase [23,32].

For natural flax fibers, the tribological behavior is more complex. Depending on the applied load used for scratching, both the contact area and the mechanical response of fibers cross-section affect the activated friction mechanisms at different scale levels as illustrated in Fig. 12. Indeed, when two surfaces are brought into contact, the role of adhesion mechanism is important at the nanoscale because the typical range of the adhesion force is in nanometers (interatomic forces) [30]. Therefore, the nano-contact area performed by the tip indenter controls the friction at nanoscale. Since the adhesion force is directly proportional to the real area of contact [30], the low applied load will generate low contact area during scratching and, then, low adhesion friction. The opposite effect occurs while scratching with a high applied load. At microscales, the mechanical indentation response is the predominant parameter as it controls the activated mechanisms that are the material shearing and deformation or plowing (see Fig. 12). In fact, when scratching with low applied load, the mechanical contact generates high elastic modulus as shown in Fig. 11. High local contact stiffness favors the material shearing and reduces the deformations [11]. When scratching with high applied load, the mechanical contact generates low elastic modulus and the opposite effect has hence occurred as illustrated in Fig. 12.

On the other hand, adhesion mechanism is predominant at nanoscale while shearing and deformation are more important at microscale (see Fig. 9). Since the considered dynamic friction is a microscopic phenomenon, the main mechanisms that control the flax fibers friction are shearing and deformation which have two reverse effects that offset each other depending on the applied load. This can explain why the flax fiber friction is not affected by the applied load increase during the scratch test.

3.4. Multiscale friction behavior of natural fibers

Section 3.2 shows that the mechanical response of flax fibers is intimately related to the geometric contact scale generated by the tip indenter radius. Since the friction behavior is dependent on the local mechanical properties (Section 3.3), the current section aims to investigate the effect of the geometric contact scale on the friction behavior of flax fibers and PP matrix to better understand the multiscale tribology of NFRP composites. Therefore, the friction behavior shown in this work will be compared to that of our previous work [23]. This latter has been performed also by scratch test with Berkovich tip indenter radius of 40 nm and an applied load range of 10 μN –30 μN . With this scratching conditions, a nanoscopic mechanical scale was performed for friction

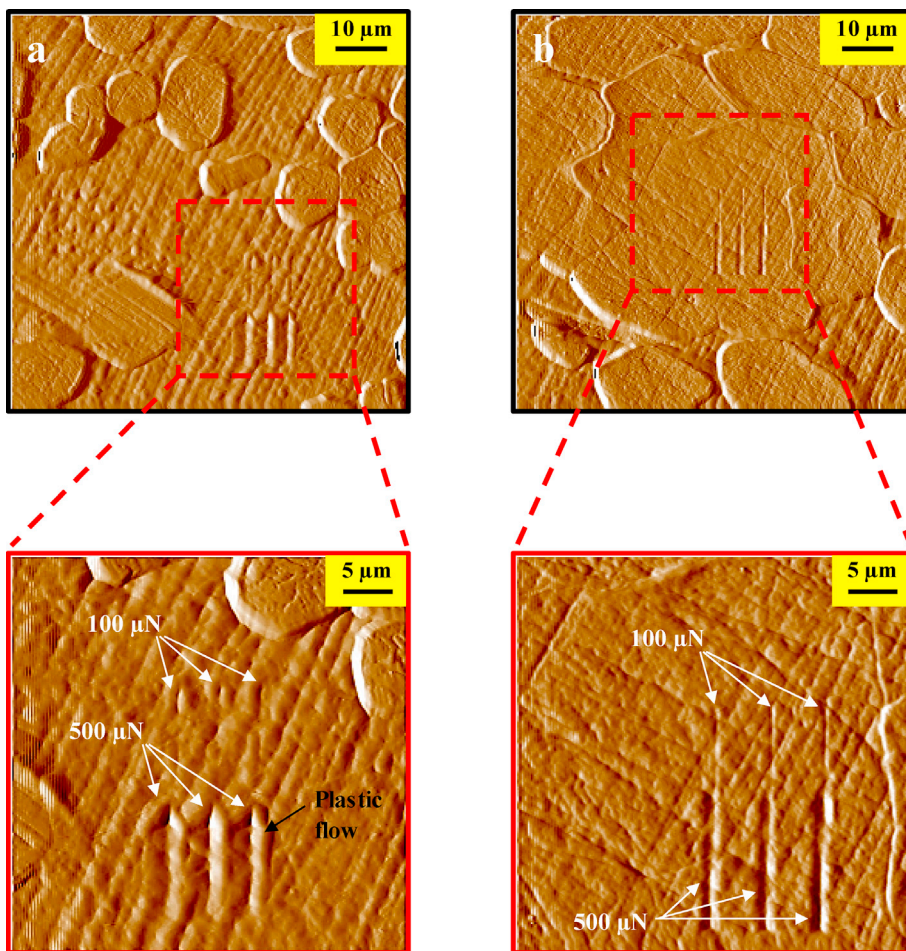


Fig. 9. SPM images showing the scratching traces on (a) PP matrix and (b) flax fiber cross-section.

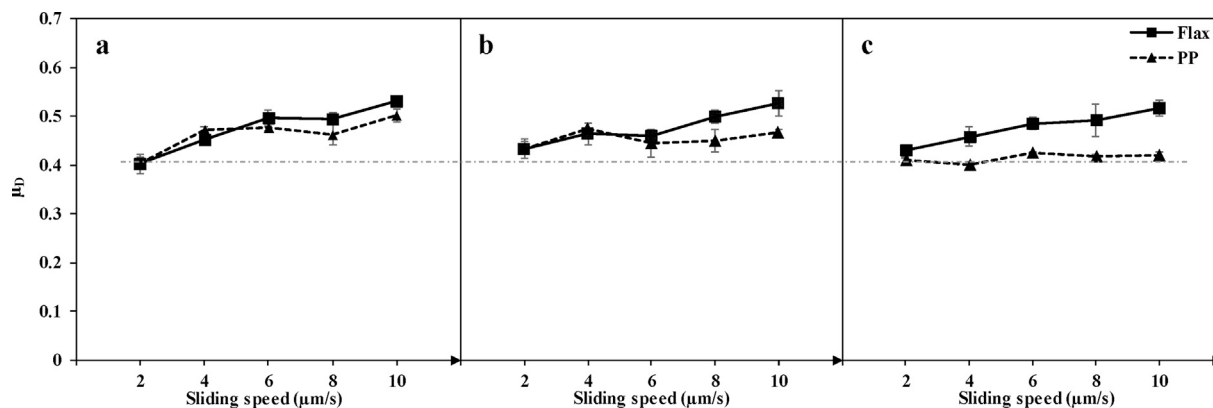


Fig. 10. Dynamic friction coefficient of flax fiber cross-section and PP matrix at different applied load: (a) 100 μN, (b) 300 μN, and (c) 500 μN.

analysis.

Fig. 13 shows that the nanoscopic friction behavior of flax fibers and PP matrix is different from their microscopic friction behavior performed in this study (Fig. 10). Indeed, unlike microscale behavior, PP matrix generates more friction than flax fibers at nanoscale. This friction difference between flax fibers and PP matrix is reduced at low sliding speed when increasing the applied load because the PP friction coefficient decreases slightly by the load increase, while the flax fibers friction coefficient increases by the load increase at low sliding speed.

The multiscale friction difference can be due to the activated friction mechanisms at nanoscale which are not similar to that of microscale. In

fact, adhesion is the predominant friction mechanism at nanoscopic contact scale as discussed in Section 3.3. For PP matrix, the friction force due to adhesion increases by increasing the applied load (i.e. increasing the contact area). However, the friction coefficient is not significantly affected by the applied load as it is the ratio between the friction force and the normal force (i.e. the applied load). Therefore, increasing both the friction force and the normal force does not affect significantly the friction coefficient.

For flax fibers, there is a supplementary phenomenon to consider that is due to the cellulosic structure of flax fibers at this scale level. Indeed, the adhesive friction presents the mechanism of energy dissipation that is

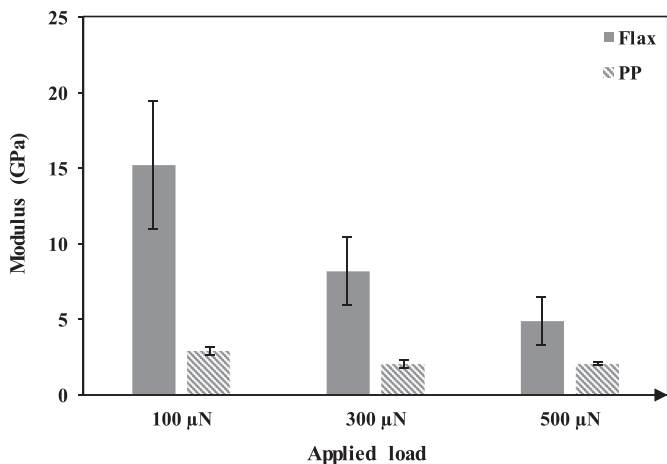


Fig. 11. Average elastic modulus obtained by nanoindentation at different applied loads.

due to both breaking strong adhesive bonds between the contacting surfaces, and the adhesion hysteresis [30]. The adhesion hysteresis has strongly occurred for heterogeneous surfaces [30]. This is the case of flax fibers cross-section that have cellulose microfibrils (1–4 nm) embedded

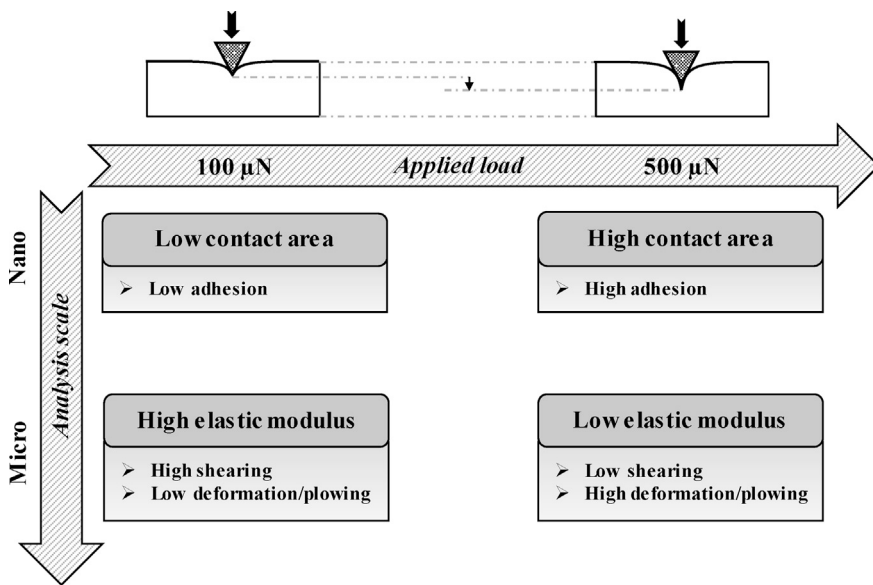


Fig. 12. Qualitative friction map of flax fibers regarding the applied load and the analysis scale.

in non-cellulosic polymers (hemicellulose and lignin). The combination of these two adhesion friction mechanisms can explain the increase of friction coefficient for flax fibers when increasing the applied load.

4. Conclusions

Multiscale tribo-mechanical analysis has been conducted on flax fibers reinforced polypropylene (PP) composites by performing nano-indentation and scratch tests. The multiscale study is made by comparing the current results to those previously realized by the authors at different geometric contact scales. The following conclusions can be drawn:

- Flax fibers stiffness shows a strong dependence on the geometric contact scale where increasing the indenter tip radius increases significantly the fiber elastic modulus. Therefore, flax fibers have multiscale mechanical properties that are intimately related to their multiscale cellulosic structure.
- The geometric contact scale is also affected by the applied normal load that change the contact area and, then, the tribo-mechanical response of flax fibers.
- PP matrix has no scale effect on its tribo-mechanical properties because of its homogeneity.

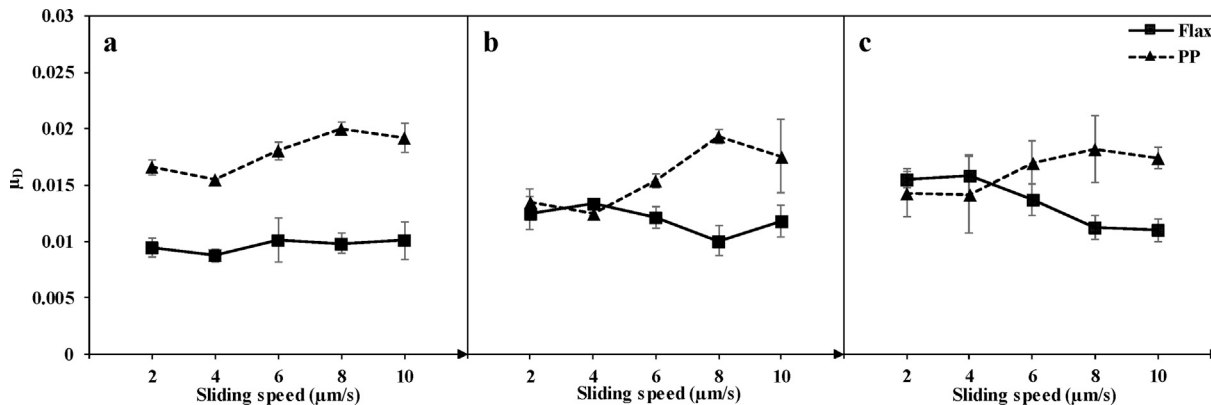


Fig. 13. Dynamic friction coefficient of flax fiber cross-section and PP matrix obtained by AFM scratch test at different applied load: (a) 10 μN, (b) 20 μN, and (c) 30 μN. Results reproduced from Ref. [23].

- The micro-friction of flax fibers is controlled by the micro-mechanical flax response that inversely affects each of shearing and plastic deformation mechanisms.
- The nano-friction of flax fibers is controlled by the heterogeneous cellulose structure of flax fibers that increases the adhesion hysteresis.

References

- [1] Omrani E, Menezes PL, Rohatgi PK. State of the art on tribological behavior of polymer matrix composites reinforced with natural fibers in the green materials world. *Eng Sci Technol Int J* 2016;19:717–36. <https://doi.org/10.1016/J.JESTCH.2015.10.007>.
- [2] Pickering KL, Aruan Efendy MG, Le TM. A review of recent developments in natural fibre composites and their mechanical performance. *Compos Part A Appl Sci Manuf* 2016;83:98–112. <https://doi.org/10.1016/J.COMPOSITESA.2015.08.038>.
- [3] Shalwan A, Yousif BF. In State of Art: mechanical and tribological behaviour of polymeric composites based on natural fibres. *Mater Des* 2013;48:14–24. <https://doi.org/10.1016/j.matdes.2012.07.014>.
- [4] Etaati A, Mehdizadeh SA, Wang H, Pather S. Vibration damping characteristics of short hemp fibre thermoplastic composites. *J Reinf Plast Compos* 2014;33:330–41. <https://doi.org/10.1177/0731684413512228>.
- [5] Rajeshkumar G, Hariharan V. Free vibration characteristics of phoenix Sp fiber reinforced polymer matrix composite beams. *Procedia Eng* 2014;97:687–93. <https://doi.org/10.1016/J.PROENG.2014.12.298>.
- [6] Alves C, Ferrao PMC, Silva AJ, Reis LG, Freitas M, Rodrigues LB, et al. Ecodesign of automotive components making use of natural jute fiber composites. *J Clean Prod* 2010;18:313–27. <https://doi.org/10.1016/J.JCLEPRO.2009.10.022>.
- [7] Ramesh M, Palanikumar K, Hemachandra Reddy K. Plant fibre based bio-composites: sustainable and renewable green materials. *Renew Sustain Energy Rev* 2017;79:558–84. <https://doi.org/10.1016/J.RSER.2017.05.094>.
- [8] Dittenber DB, GangaRao HVS. Critical review of recent publications on use of natural composites in infrastructure. *Compos Part A Appl Sci Manuf* 2012;43:1419–29. <https://doi.org/10.1016/j.compositesa.2011.11.019>.
- [9] Shah DU. Developing plant fibre composites for structural applications by optimising composite parameters: a critical review. *J Mater Sci* 2013;48:6083–107. <https://doi.org/10.1007/s10853-013-7458-7>.
- [10] Davim JP, Reis P. Damage and dimensional precision on milling carbon fiber-reinforced plastics using design experiments. *J Mater Process Technol* 2005;160:160–7. <https://doi.org/10.1016/j.jmatprotec.2004.06.003>.
- [11] Chegdani F, Mezghani S, El Mansori M, Mkaddem A. Fiber type effect on tribological behavior when cutting natural fiber reinforced plastics. *Wear* 2015;332–333:772–9. <https://doi.org/10.1016/j.wear.2014.12.039>.
- [12] Chegdani F, Mezghani S, El Mansori M. On the multiscale tribological signatures of the tool helix angle in profile milling of woven flax fiber composites. *Tribol Int* 2016;100:132–40. <https://doi.org/10.1016/j.triboint.2015.12.014>.
- [13] Chegdani F, Mezghani S, El Mansori M. Experimental study of coated tools effects in dry cutting of natural fiber reinforced plastics. *Surf Coating Technol* 2015;284:264–72. <https://doi.org/10.1016/j.surfcoat.2015.06.083>.
- [14] Chegdani F, Mezghani S, El Mansori M. Correlation between mechanical scales and analysis scales of topographic signals under milling process of natural fibre composites. *J Compos Mater* 2017;51:2743–56. <https://doi.org/10.1177/0021998316676625>.
- [15] Baley C. Analysis of the flax fibres tensile behaviour and analysis of the tensile stiffness increase. *Compos - Part A Appl Sci Manuf* 2002;33:939–48. [https://doi.org/10.1016/S1359-835X\(02\)00040-4](https://doi.org/10.1016/S1359-835X(02)00040-4).
- [16] Lefevre A, Bourmaud A, Lebrun L, Morvan C, Baley C. A study of the yearly reproducibility of flax fiber tensile properties. *Ind Crop Prod* 2013;50:400–7. <https://doi.org/10.1016/j.indcrop.2013.07.035>.
- [17] Yousif BF, Lau STW, McWilliam S. Polyester composite based on betelnut fibre for tribological applications. *Tribol Int* 2010;43:503–11. <https://doi.org/10.1016/J.TRIBOINT.2009.08.006>.
- [18] Nirmal U, Hashim J, Low KO. Adhesive wear and frictional performance of bamboo fibres reinforced epoxy composite. *Tribol Int* 2012;47:122–33. <https://doi.org/10.1016/J.TRIBOINT.2011.10.012>.
- [19] Bakry M, Mousa MO, Ali WY. Friction and wear of friction composites reinforced by natural fibres. *Mater Werkst* 2013;44:21–8. <https://doi.org/10.1002/mawe.201300962>.
- [20] Yallev TB, Kumar P, Singh I. Sliding wear properties of jute fabric reinforced polypropylene composites. *Procedia Eng* 2014;97:402–11. <https://doi.org/10.1016/J.PROENG.2014.12.264>.
- [21] Nirmal U, Hashim J, Megat Ahmed MMH. A review on tribological performance of natural fibre polymeric composites. *Tribol Int* 2015;83:77–104. <https://doi.org/10.1016/J.TRIBOINT.2014.11.003>.
- [22] Bajpai PK, Singh I, Madaan J. Tribological behavior of natural fiber reinforced PLA composites. *Wear* 2013;297:829–40. <https://doi.org/10.1016/J.WEAR.2012.10.019>.
- [23] Chegdani F, El Mansori M, Mezghani S, Montagne A. Scale effect on tribo-mechanical behavior of vegetal fibers in reinforced bio-composite materials. *Compos Sci Technol* 2017;150:87–94. <https://doi.org/10.1016/j.compscitech.2017.07.012>.
- [24] Oliver WC, Pharr GM. An improved technique for determining hardness and elastic-modulus using load and displacement sensing indentation experiments. *J Mater Res* 1992;7:1564–83. <https://doi.org/10.1557/>.
- [25] Buckley CP. Origin of nonlinear viscoelastic effects in polypropylene. *J Phys D Appl Phys* 1977;10:2135–53. <https://doi.org/10.1088/0022-3727/10/15/017>.
- [26] Drozdov AD. Effect of temperature on the viscoelastic and viscoplastic behavior of polypropylene. *Mech Time-Dependent Mater* 2010;14:411–34. <https://doi.org/10.1007/s11043-010-9118-5>.
- [27] Keryvin V, Lan M, Bourmaud A, Parenteau T, Charleux L, Baley C. Analysis of flax fibres viscoelastic behaviour at micro and nano scales. *Compos Part A Appl Sci Manuf* 2015;68:219–25. <https://doi.org/10.1016/j.compositesa.2014.10.006>.
- [28] Bos HL, Molenveld K, Teunissen W, van Wingerde AM, van Delft DRV. Compressive behaviour of unidirectional flax fibre reinforced composites. *J Mater Sci* 2004;39:2159–68. <https://doi.org/10.1023/B:JMSE.0000017779.08041.49>.
- [29] Youssefian S, Rahbar N. Molecular origin of strength and stiffness in bamboo fibrils. *Sci Rep* 2015;5:11116. <https://doi.org/10.1038/srep11116>.
- [30] Nosonovsky M, Bhushan B. Multiscale friction mechanisms and hierarchical surfaces in nano- and bio-tribology. *Mater Sci Eng R Rep* 2007;58:162–93. <https://doi.org/10.1016/J.MSER.2007.09.001>.
- [31] Chegdani F, El Mansori M. Friction scale effect in drilling natural fiber composites. *Tribol Int* 2018;119:622–30. <https://doi.org/10.1016/j.triboint.2017.12.006>.
- [32] Gracias DH, Somorjai GA. Continuum force microscopy study of the elastic modulus, hardness and friction of polyethylene and polypropylene surfaces. *Macromolecules* 1998;31:1269–76. <https://doi.org/10.1021/ma970683b>.